Parametric Methods for Order Tracking Analysis

Nielsen, Jesper Kjær; Jensen, Tobias Lindstrøm

Publication date:
2017

Document Version
Publisher's PDF, also known as Version of record

Parametric Methods for Order Tracking Analysis

Jesper Kjær Nielsen and Tobias Lindstrøm Jensen
Aalborg University

Initial: November 24, 2015; Last compiled: June 26, 2017

Contents

Abstract

Order tracking analysis is often used to find the critical speeds at which structural resonances are excited by a rotating machine. Typically, order tracking analysis is performed via non-parametric methods. In this report, however, we demonstrate some of the advantages of using a parametric method for order tracking analysis. Specifically, we show that we get a much better time and frequency resolution, obtain a much more robust and accurate estimate of the RPM profile, and are able to perform accurate order tracking analysis even without the tachometer signal.

Introduction

Order tracking is an important tool for the analysis of vibrational or acoustical signals originating from rotating machines [1]. The analysis of such rotating machines is used to determine the critical speeds where structural resonances are excited by the rotation of the machine. Therefore, the analysis is often carried out by accelerating (run-up) and decelerating (coast-down) the machine under test while recording the vibrational or acoustical signals.

For a constant rotation frequency, rotating machines produce approximately periodic signals which can be modelled as

$$x(t) = \sum_{i=1}^{l} A_i \cos(i\Omega_0 t + \phi_i) + e(t) \tag{1}$$

where A_i and ϕ_i are the amplitude and phase of the i'th harmonic component (or order), Ω_0 is the fundamental frequency in radians per second, and $e(t)$ is additive noise. The rotation frequency r is related to the fundamental frequency via

$$r = 60\frac{\Omega_0}{2\pi} = 60 f_0 \tag{2}$$

and is measured in revolutions per minute (RPM) (f_0 is measured in Hz). Given these definitions, we can now state how the analysis of rotating machines can be carried out.

> Given a vibrational or acoustical signal, estimate the amplitudes and phases of every harmonic component (or order) as a function of the rotation frequency.

The classical way of doing the above analysis is to compute a spectrogram which shows the magnitude spectrum of the signals as a function of time and frequency. The main problem of this approach is the smearing of the spectrum which occurs at especially the higher harmonics when the rotation frequency is time varying [1]. This problem is caused by the intrinsic trade-off between time- and frequency resolution.

To avoid the problem of smearing, a resampling technique can be used in which the vibrational or acoustical signals are sampled relative to the rotation frequency [1,2]. That is, we sample uniformly in angle instead of in time and get a number of samples per revolution instead of per second. For this sampling technique, the plot equivalent to the spectrogram is referred to as the order spectrum, and it shows the magnitude spectrum of the signals as a function of rotation frequency and order. The harmonic components will show up as vertical lines in the order spectrum and smearing is no longer a problem, even for the higher harmonics.

In order to do the resampling, the rotation frequency must be estimated accurately. This is called tracking. Traditionally, this has been performed with a tachometer which generates one or several pulses for every rotation. Since it might be difficult and/or expensive to mount such a tachometer close to the rotating parts of the machines, methods for estimating the rotation frequency directly from the vibrational or acoustical signals have also been proposed [3]. Such methods are generally referred to as autotrackers.

Parametric Order Tracking Analysis

Surprisingly, only a few parametric methods for order tracking analysis have been proposed. According to [2], parametric order tracking methods have so far been used with only a limiting success with the most promising one being the Vold-Kalman filter method [4]. Although we are far from being experts within the application domain of order tracking analysis, we believe that parametric methods can give a number of advantages that are not possible using non-parametric methods. Some of these are listed below.

- If the tachometer signal is unavailable, the rotation frequency can be estimated directly from the recordings.
- The time and frequency resolution become much better.
- There is no need to do tachometer-based resampling of the signals due to the increase time and frequency resolution. Moreover, run-ups and coast-downs can also be included in the model.
- A raw tachometer signal is also a periodic signal which can be analysed using a parametric autotracker. This is much more accurate and robust than measuring trigger level crossings as suggested in [2].
- There is no need to first estimate the rotation frequency from a tachometer signal and then use this estimate in the order analysis. Instead, the two steps can be combined in a multichannel estimator, and this increases the robustness to errors in the raw tachometer signal.
- On a related note, data from multiple sensors can be used for order tracking. Sensor arrays also allow us to filter out noise sources spatially.
- The results of a parametric analysis can be used as an aid in non-parametric analysis.
- The number of user parameters is much smaller.

In the rest of this report, we will demonstrate some of these points.

Signal Model

We attack the problem in a similar way to what was suggested in [3, 5]. Thus, we model the vibrational or acoustical signal as being a uniformly sampled and periodic signal in additive noise $e(n)$ given by

$$x(n) = \sum_{i=1}^{l} [a_i \cos(i\omega_0(n)n) - b_i \sin(i\omega_0(n)n)] + e(n) \tag{3}$$

$$= \sum_{i=1}^{l} A_i \cos(i\omega_0(n)n + \phi_i) + e(n) \tag{4}$$

where a_i and b_i are the linear weights, A_i is the amplitude, and ϕ_i is the phase of the i'th harmonic component. Moreover, $\omega_0(n)$ is the fundamental frequency in radians per sample which we have made time-varying so that we can model run ups and coast downs. Specifically, we consider the two models

$$\omega_0(n) = \omega_0 \tag{5}$$
$$\omega_0(n) = \omega_0 + \beta_0 n \tag{6}$$

where the former is a special case of the latter. In the derivation in this section, we therefore focus on the latter where the chirp rate parameter β_0 models a linear increase or decrease in the fundamental frequency during a segment. Note that this linear model of the fundamental frequency can be viewed as a first order Taylor approximation to $\omega_0(n)$ which is usually fairly accurate if the segment length is not too long.

If an N-dimensional data set $\{x(n)\}_{n=n_0}^{n_0+N-1}$ is observed, the signal model can be written in vector form as

$$\boldsymbol{x} = \boldsymbol{H}_l(\omega_0, \beta_0)\boldsymbol{\alpha}_l + \boldsymbol{e} \tag{7}$$

where

$$\boldsymbol{x} = \begin{bmatrix} x(n_0) & \cdots & x(n_0+N-1) \end{bmatrix}^T \tag{8}$$
$$\boldsymbol{e} = \begin{bmatrix} e(n_0) & \cdots & e(n_0+N-1) \end{bmatrix}^T \tag{9}$$
$$\boldsymbol{c}(\omega,\beta) = \begin{bmatrix} \cos(\omega n_0 + \beta n_0^2) & \cdots & \cos(\omega(n_0+N-1) + \beta(n_0+N-1)^2) \end{bmatrix}^T \tag{10}$$
$$\boldsymbol{s}(\omega,\beta) = \begin{bmatrix} \sin(\omega n_0 + \beta n_0^2) & \cdots & \sin(\omega(n_0+N-1) + \beta(n_0+N-1)^2) \end{bmatrix}^T \tag{11}$$
$$\boldsymbol{C}_l(\omega_0,\beta_0) = \begin{bmatrix} \boldsymbol{c}(\omega_0,\beta_0) & \cdots & \boldsymbol{c}(l\omega_0, l\beta_0) \end{bmatrix} \tag{12}$$
$$\boldsymbol{S}_l(\omega_0,\beta_0) = \begin{bmatrix} \boldsymbol{s}(\omega_0,\beta_0) & \cdots & \boldsymbol{s}(l\omega_0, l\beta_0) \end{bmatrix} \tag{13}$$
$$\boldsymbol{H}_l(\omega_0,\beta_0) = \begin{bmatrix} \boldsymbol{C}_l(\omega_0,\beta_0) & \boldsymbol{S}_l(\omega_0,\beta_0) \end{bmatrix} \tag{14}$$
$$\boldsymbol{a}_l = \begin{bmatrix} a_1 & \cdots & a_l \end{bmatrix}^T \tag{15}$$
$$\boldsymbol{b}_l = \begin{bmatrix} b_1 & \cdots & b_l \end{bmatrix}^T \tag{16}$$
$$\boldsymbol{\alpha}_l = \begin{bmatrix} \boldsymbol{a}_l^T & -\boldsymbol{b}_l^T \end{bmatrix}^T \tag{17}$$

where n_0 is the start index which is usually set as $n_0 = 0$. When the noise is white and Gaussian, the maximum likelihood (ML) estimator of ω_0 and β_0 is

$$(\hat{\omega}_0, \hat{\beta}_0) = \underset{\omega_0,\beta_0}{\operatorname{argmax}}\, \boldsymbol{x}^T \boldsymbol{H}_l(\omega_0,\beta_0) \left[\boldsymbol{H}_l^T(\omega_0,\beta_0)\boldsymbol{H}_l(\omega_0,\beta_0)\right]^{-1} \boldsymbol{H}_l^T(\omega_0,\beta_0)\boldsymbol{x}\ . \tag{18}$$

The ML estimator is a statistically efficient estimator if enough data are available. That is, it is the most accurate estimator when the signal model holds. For the model with $\beta_0 = 0$, we have developed an algorithm that significantly reduces this cost [6–8]. There

are also recent developments for the case $\beta_0 \neq 0$ [9,10]. The results presented in the rest of this report is only based on the model with $\beta_0 = 0$. Besides the fundamental frequency and the chirp rate, the number of harmonics (the model order) is also unknown. We also estimate this based on our previous work in [11,12].

Key Points

The rest of this report is divided into four sections. In the first three, we demonstrate the following.

- *Washing Machine Engine:*
  Using a recording from a washing machine engine, we demonstrate the time and frequency resolution that a parametric method can give, even at a low sampling frequency and with no tachometer signal.

- *Car Engines:*
  In contrast to the rotation frequency of the washing machine engine, the rotation frequencies of the car engines change as a function of time. Despite this, the ML estimator based on the model with a constant rotation frequency still gives good and high resolution results. Moreover, we demonstrate for an engine signal we can estimate the rotation speed almost as accurately from the recordings than B&K PULSE Reflex software can from the tachometer signal with tuned parameter settings and smoothing.

- *Tachometer Signal Analysis:*
  Based on a simulated tachometer signal, we show how accurately we can estimate the RPM profile for various SNRs and for both Gaussian and Laplacian noise. The latter is much more impulsive in nature than the former.

In the fourth and final section, we summarise our main findings and list a number of things that would be interesting to look more into.

Washing Machine Engine

We first consider the analysis of a single channel recording of a washing machine. To have a visual understanding of the parametric fundamental frequency analyser, we show a spectrogram of the signal. We will then overlay this spectrogram with some of the information extracted from the parametric method. Such an example is shown in Fig. 1. The settings for the parametric fundamental frequency analyser is:

- Fundamental frequency bounds $f_0 \in [30, 1000]$ [Hz].
- Downsampling factor $Q = 8$ ($f_s = 44100 \rightarrow 5512.5$ [Hz])
- Max model order $L = 15$.
- Frame size $N = 256$ samples (~ 0.046 [s]). (box-car processing)

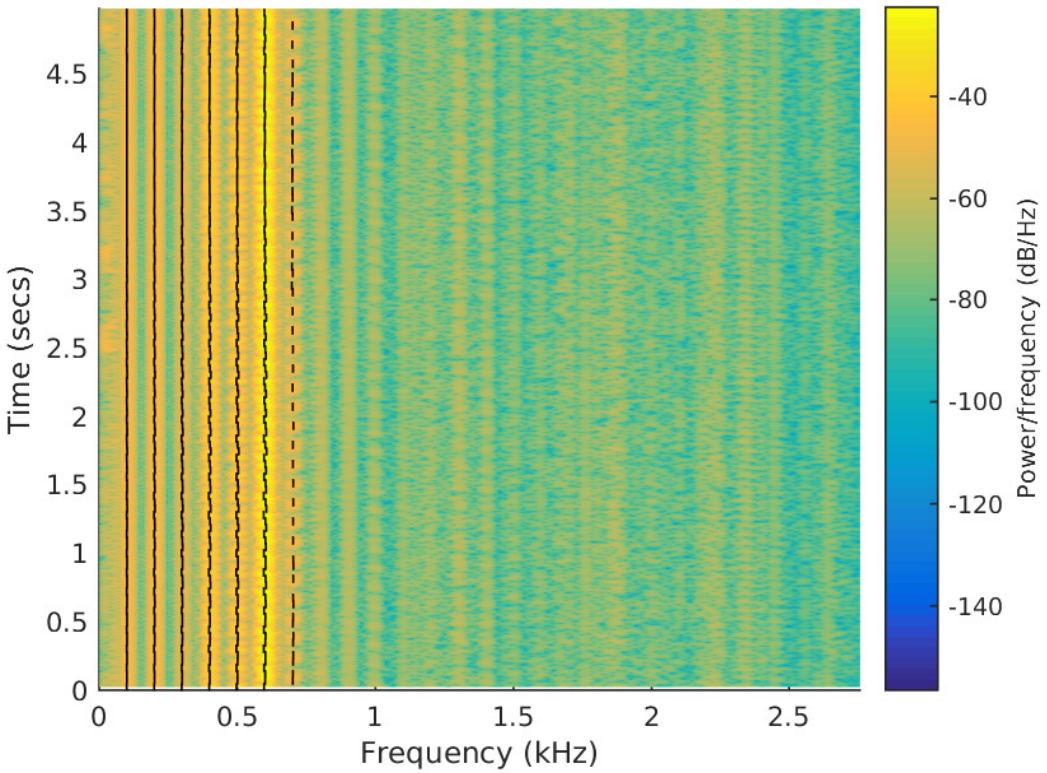

Figure 1: Spectrogram of a washing machine engine audio recording. Settings: 2048 sample Hann window, 2000 sample overlap, $N_{\text{FFT}} = 8192$. The black lines indicates the fundamental frequency and overtones for the harmonic signal at the given time.

We observe the following from Fig. 1:

1. The rotation frequency of the washing machine modulates. This is hard to see from the spectrogram, but the parametric estimator clearly reveals that.

2. The estimated model order varies between 6 and 7. The 7th harmonic component is not constantly present, but has an on/off behavior across time. This can also be seen in the spectrogram.

3. The 6th harmonic component is the strongest harmonic component.

The estimated fundamental frequency is shown as a function of time in Fig. 2. From the figure, we see that the harmonic model has approximately a constant fundamental frequency with a slight modulation in the order of 7 [Hz/s].

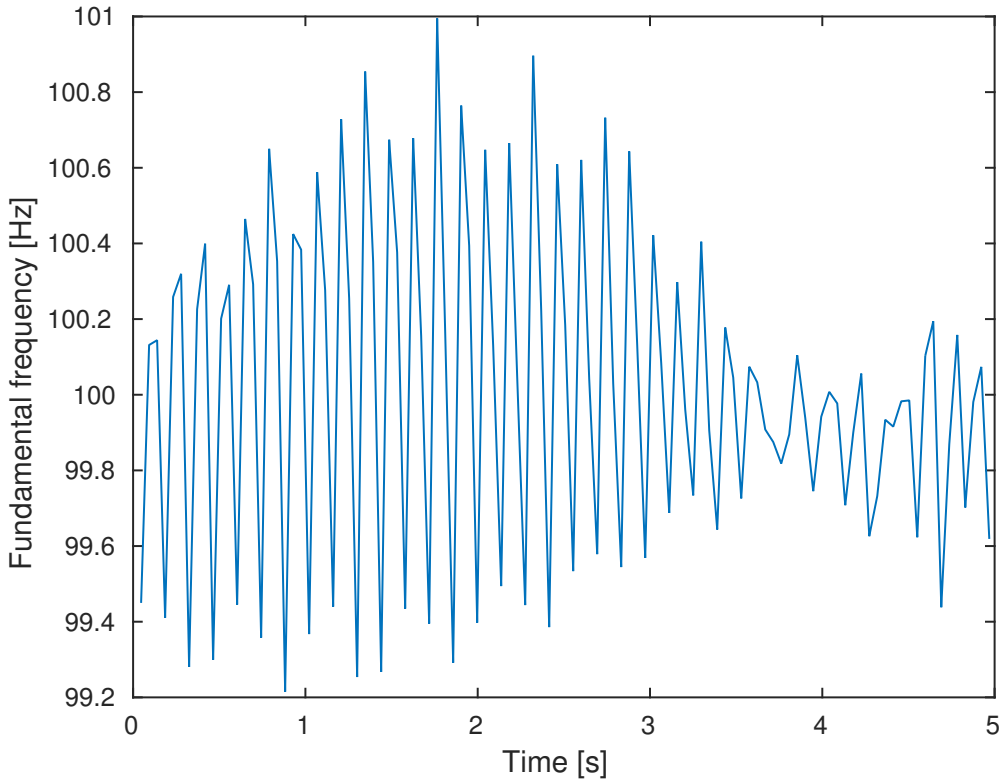

Figure 2: Estimated fundamental frequency as a function of time.

From the parametric harmonic model, we may also inspect the power of the individual harmonics as a function of time. Note that this is not done using any frequency analysis

tools, but is simply obtained as

$$p_i = \frac{1}{N} \sum_{n=n_0}^{n_0+N-1} \left(a_i \cos(i\omega_0 n) - b_i \sin(i\omega_0 n)\right)^2 \tag{19}$$

$$= \frac{1}{2} a_i^2 \left(1 + \frac{\sin(\omega_0 i N)}{N \sin(\omega_0 i)}\right) + \frac{1}{2} b_i^2 \left(1 - \frac{\sin(\omega_0 i N)}{N \sin(\omega_0 i)}\right) \tag{20}$$

with symmetric time index $n_0 = -\frac{N-1}{2}$. Note that $p_i \simeq \frac{1}{2}(a_i^2 + b_i^2)$. This is shown in Fig. 3. From Fig. 3 we observe that there is most power in the 6th harmonic component and that the 7th harmonic component is not always present.

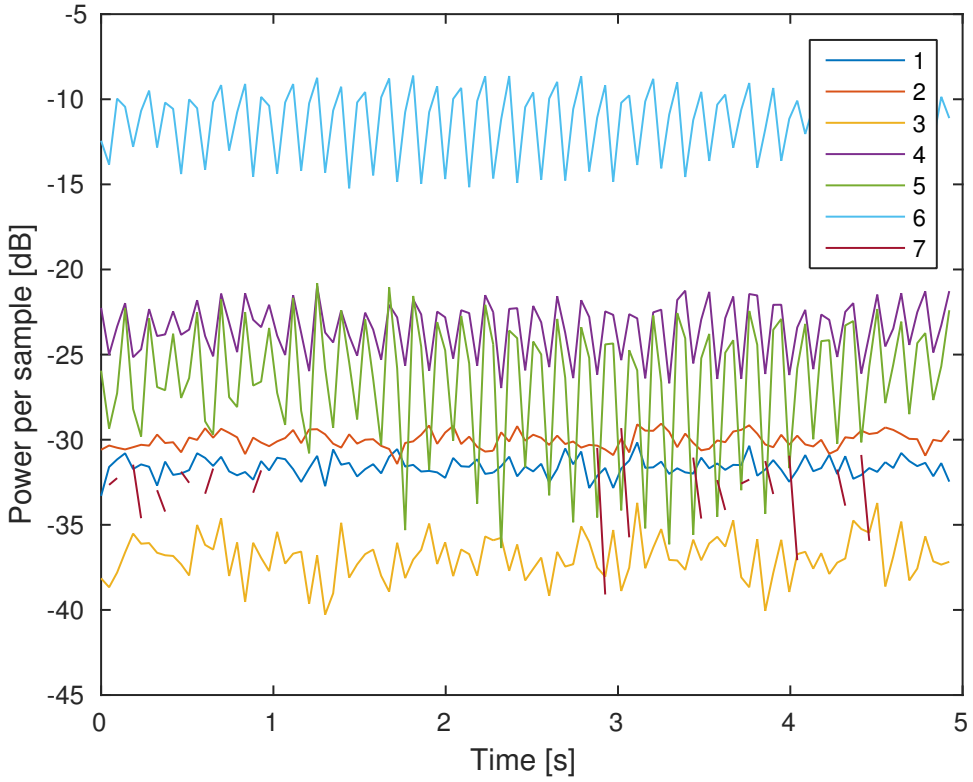

Figure 3: Estimated power of the individual harmonics as a function of time. Notice that there is most power in the harmonic $i = 6$.

From a computational side, the ML estimates were computed using a Matlab implementation in approximately 4 [s] on a standard laptop (Intel(R) Core(TM) i7-5600U CPU @ 2.60GHz, 8GB DDR3 RAM @ 1.6GHz). For comparison, the spectrogram was computed in approximately 0.45 [s]. If we instead changed the settings to $L = 10$ and fundamental frequency bounds of $f_0 \in [30, 300]$, the ML estimates were computed in 1.8 [s].

An even better time and frequency resolution can be obtained by using overlapping frames. To accommodate this, we change the settings of the parametric fundamental frequency analyser to:

- Fundamental frequency bounds $f_0 \in [75, 150]$ [Hz].
- Downsampling factor $Q = 8$ ($f_s = 44100 \to 5512.5$ [Hz])
- Max model order $L = 15$.
- Frame size $N = 256$ samples (~ 0.046 [s]) with $o = 250$ overlap.

The overlayed spectrogram, estimated fundamental frequency and harmonic power versus time are shown in Fig. 4, 5, 6, respectively. Note the high resolution in both time and frequency which reveals details that are not possible to see in a spectrogram.

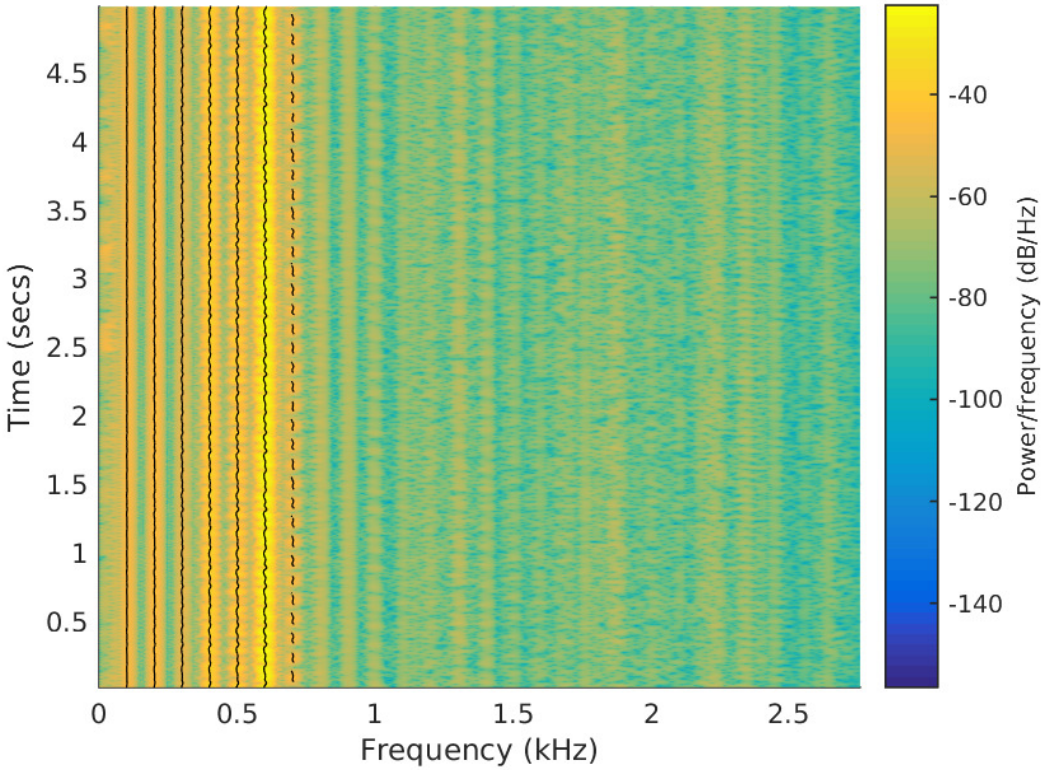

Figure 4: Spectrogram of a washing machine engine audio recording. Settings: 2048 sample Hann window, 2000 sample overlap, $N_{\text{FFT}} = 8192$. The black lines indicates the fundamental frequency and overtones for the harmonic signal at the given time using overlap $o = 250$ and $N = 256$.

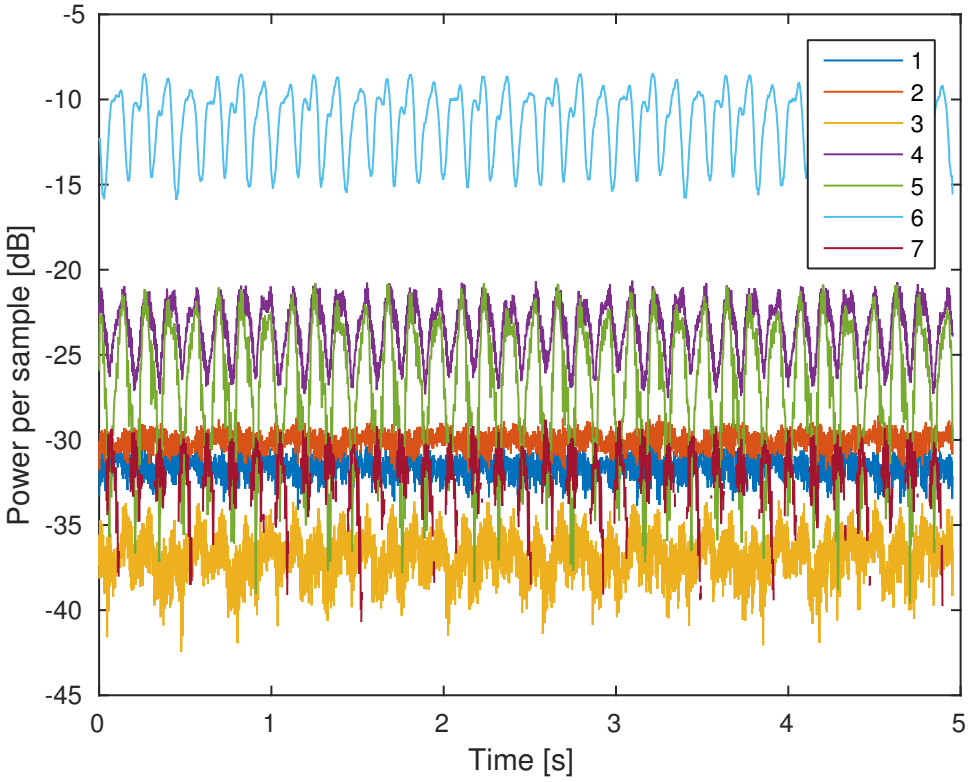

Figure 5: Estimated power of the individual harmonics as a function of time. $o = 250$ and $N = 256$.

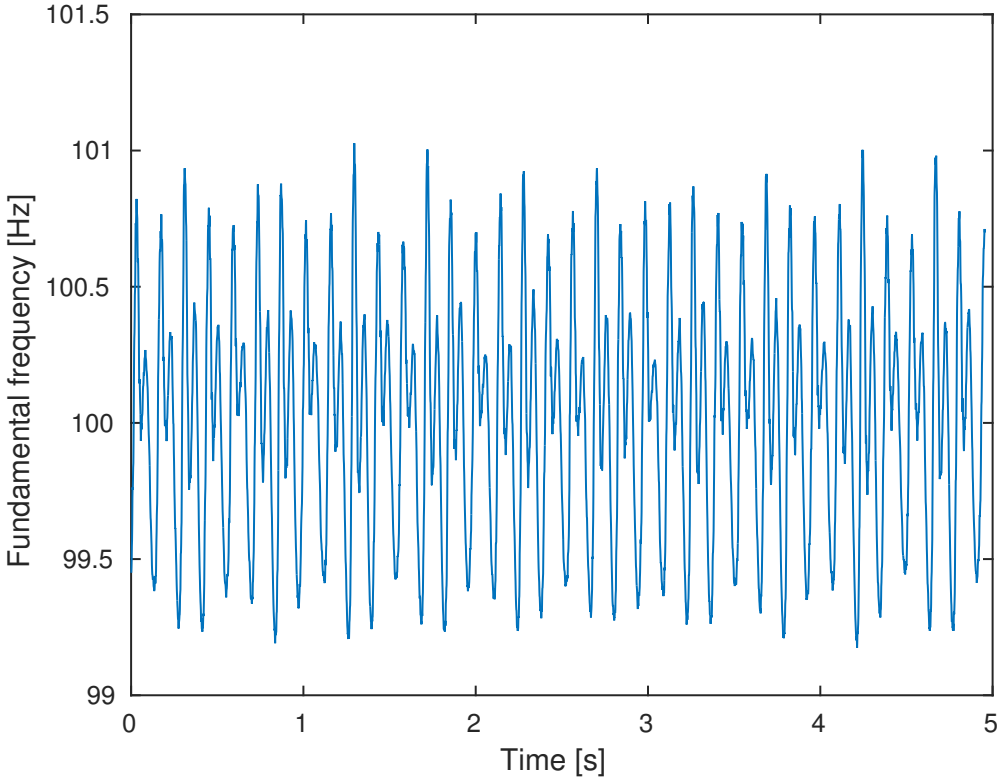

Figure 6: Estimated fundamental frequency as a function of time. $o = 250$ and $N = 256$.

Car Engines

Car Engine I

In this example we consider the analysis of a two channel recording of a car acceleration and deacceleration. The initial settings for the parametric fundamental frequency analyser is:

- Select the first channel.
- Fundamental frequency bounds $f_0 \in [20, 100]$ [Hz].
- Downsampling factor $Q = 16$ ($f_s = 32768 \to 2048$ [Hz])
- Max model order $L = 10$.
- Frame size $N = 256$ samples (~ 0.125 [s]). (box-car processing)
- High-pass fourth order Chebyshev Type I filter with cutoff frequency 50 [Hz] to remove noise from tyres.

The overlayed spectrogram and estimated fundamental frequency is shown in Fig. 7 and 8. From the trends observed in these figures, we may expect that the fundamental frequency actually is in the bound $f_0 \in [20, 60]$ [Hz] for the observed signal and that we could increase the frame size to $N = 512$. Notice that we are actually estimating a fundamental frequency of a harmonic signal where the fundamental frequency has been removed by a high-pass filter. With these new settings we obtain the overlayed spectrogram in Fig. 9 and 10. With these settings, we observe a much smoother (as expected) ascend and descend of the fundamental frequency. This will be an example of a workflow for an engineer or general user that will use a parametric fundamental frequency analyser.

Car Engine II

In this example we consider the analysis of a two channel recording of a car engine acceleration Here we can compare the estimated fundamental frequency with an estimated RPM profile from a tachometer. The settings for the parametric fundamental frequency analyser is:

- Select the first channel.
- Fundamental frequency bounds $f_0 \in [15, 60]$ [Hz].
- Downsampling factor $Q = 16$ ($f_s = 44100 \to 2756.2$ [Hz])
- Max model order $L = 20$.
- Frame size $N = 512$ samples (~ 0.185 [s]). (box-car processing)

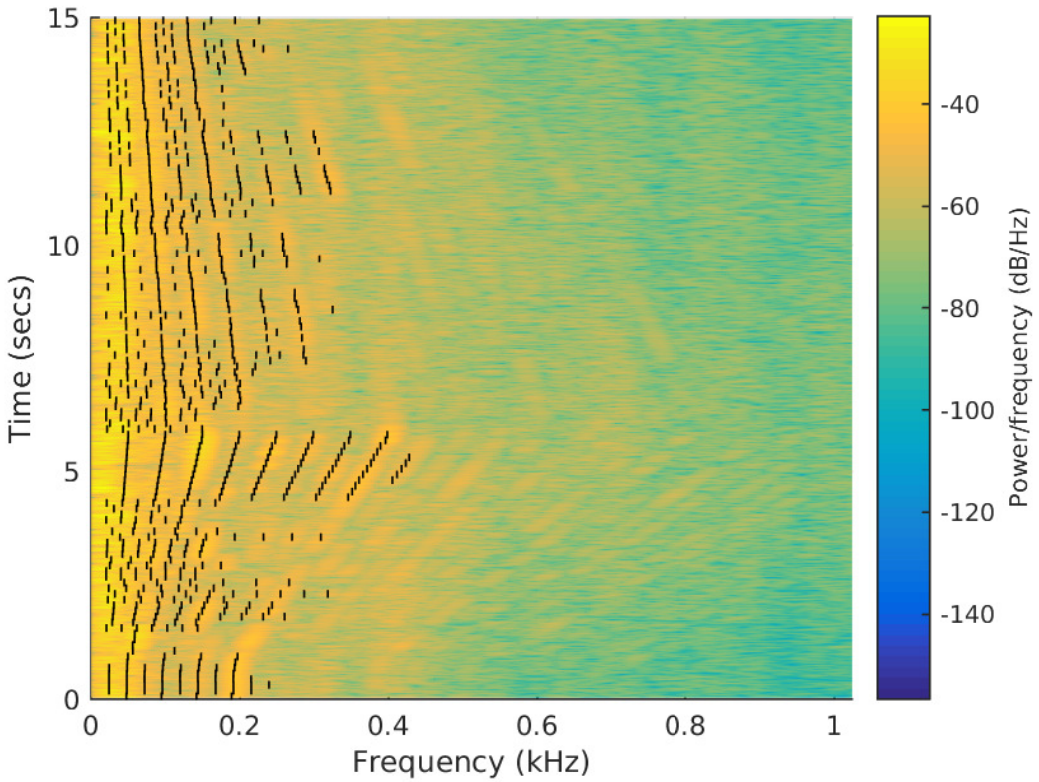

Figure 7: Spectrogram of a car engine acceleration and deacceleration. Settings: 2048 sample Hann window, 2000 sample overlap, $N_{\text{FFT}} = 8192$. The black lines indicates the fundamental frequency and overtones for the harmonic signal at the given time.

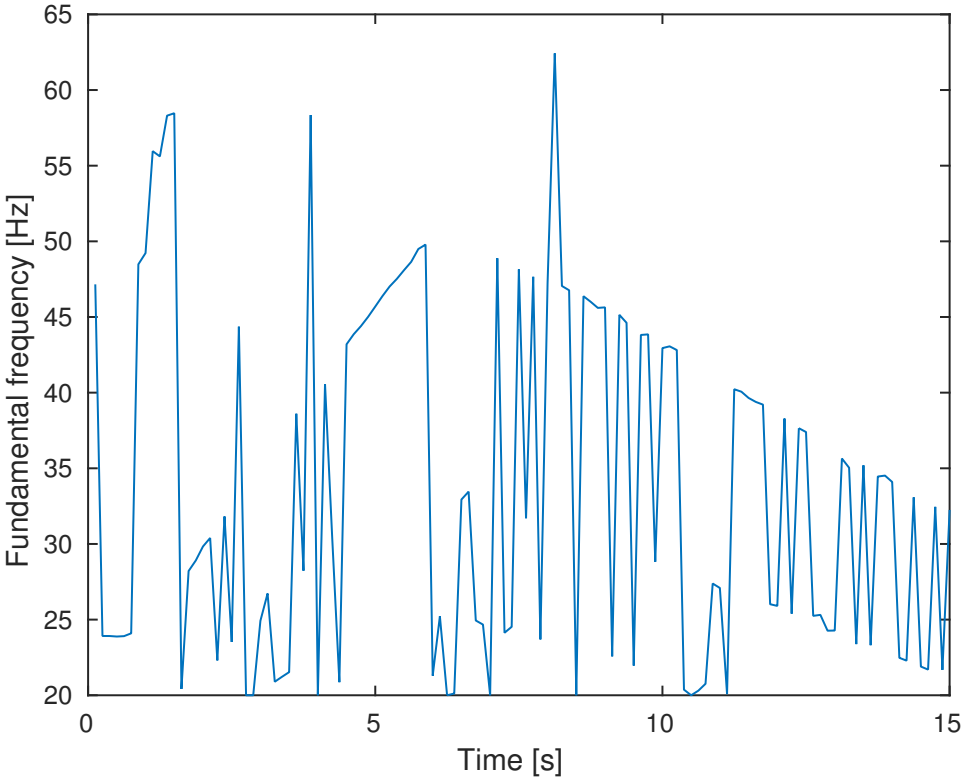

Figure 8: Estimated fundamental frequency as a function of time.

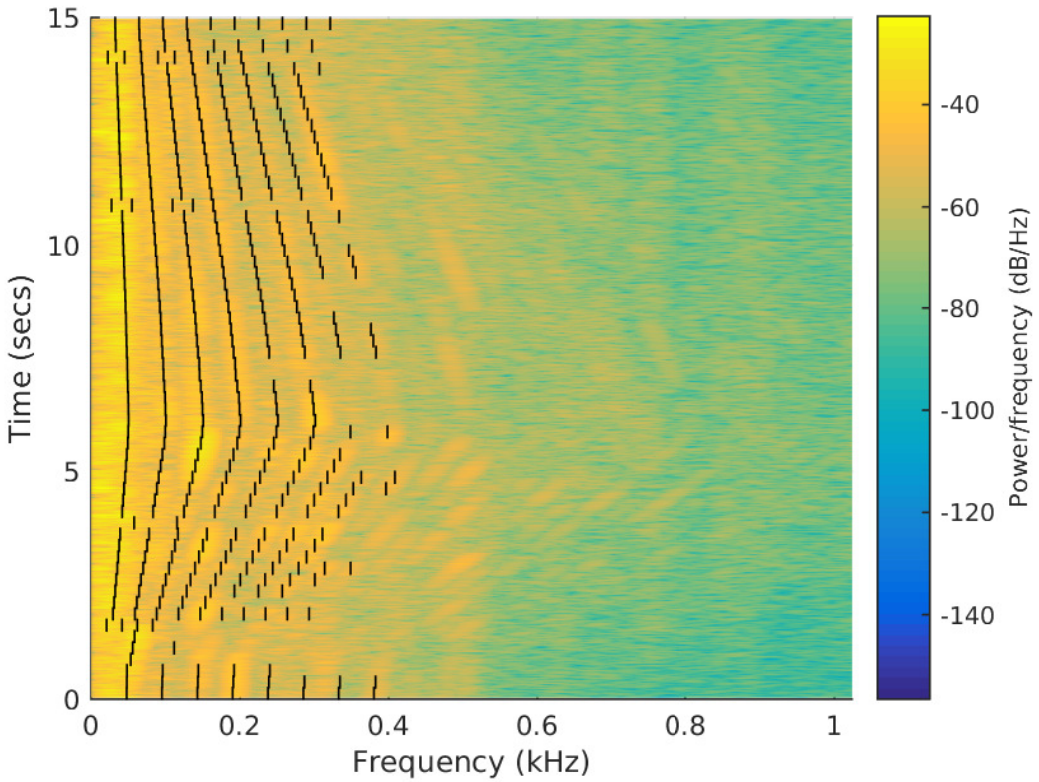

Figure 9: Spectrogram of a car engine acceleration and deacceleration. Settings: 2048 sample Hann window, 2000 sample overlap, $N_{\text{FFT}} = 8192$. The black lines indicates the fundamental frequency and overtones for the harmonic signal at the given time. Second setup.

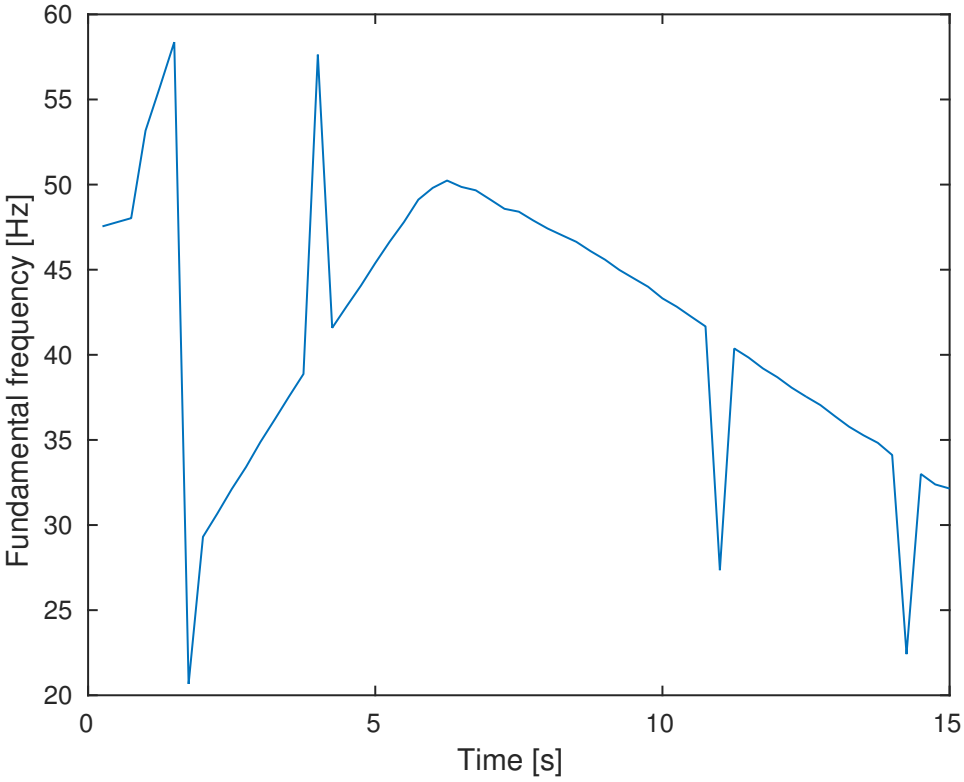

Figure 10: Estimated fundamental frequency as a function of time. Second setup.

- High-pass fourth order Chebyshev Type I filter with cutoff frequency 200 [Hz] to remove noise from tyres.

The overlayed spectrogram is shown in Fig. 11. We observe the acceleration trend in both the spectrogram and overlayed parametric information. The estimated model order changes over time depending on whether enough energy is present in higher order harmonics. Notice that we again are actually estimating a fundamental frequency of a harmonic signal where the fundamental frequency and several harmonics has been removed by the high-pass filter. The estimated fundamental frequency using the acoustic signal and parametric as well as RPM profiles obtained via tacho signals are shown in Fig. 12. The trigger based estimator (see Fig. 16) runs on the binary tacho signal in the LSB of channel 2 using a simple trigger. The PULSE Reflex RPM profile is a processed RPM profile using the PULSE Reflex software (in default settings) and one in tuned setting with smoothing. We observe that the estimated fundamental frequency using the parametric method for an acoustic channel follows the trend of the trigger based estimator. As in the example with the washing machine engine, we might also

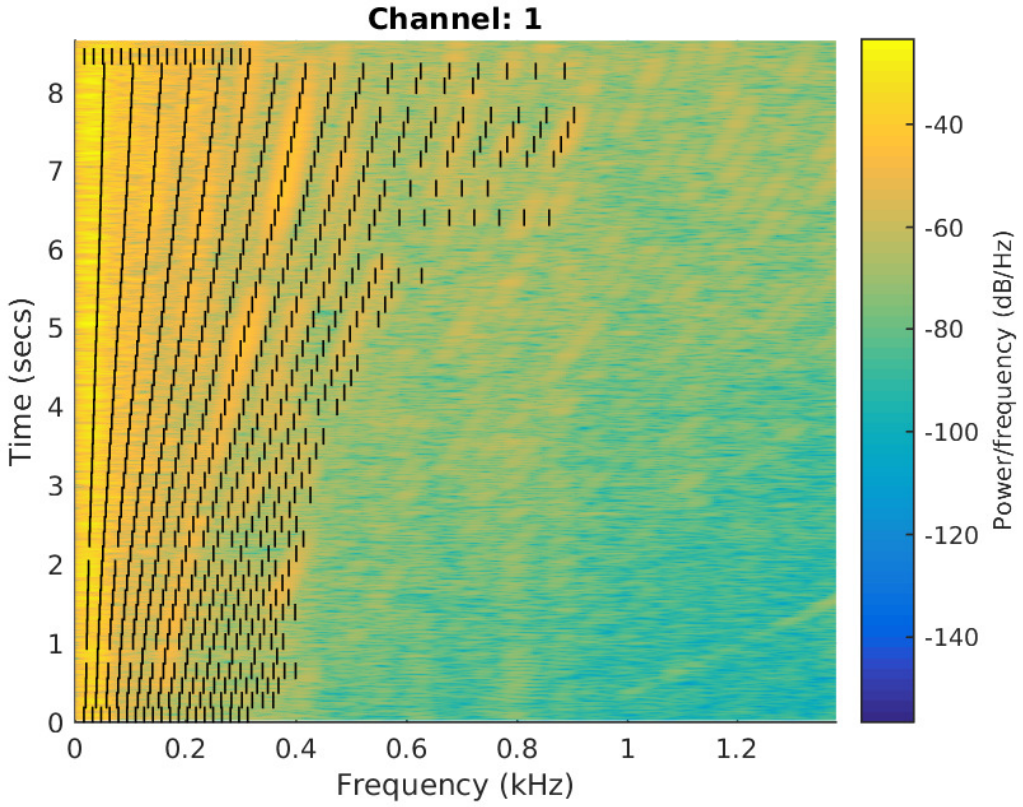

Figure 11: Spectrogram of a car engine acceleration. Settings: 2048 sample Hann window, 2000 sample overlap, $N_{\text{FFT}} = 8192$. The black lines indicates the fundamental frequency and overtones for the harmonic signal at the given time.

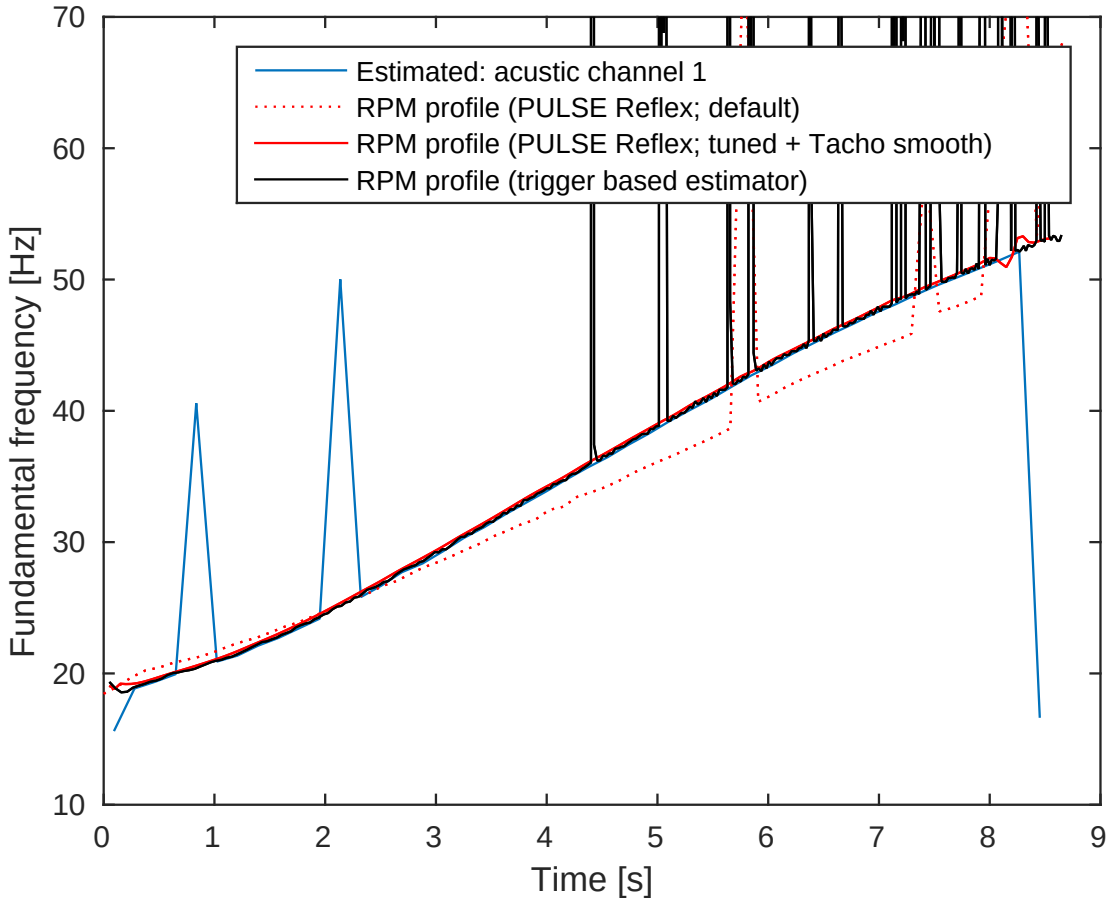

Figure 12: Estimated fundamental frequency as a function of time from the acoustic signal via the parametric method as well as RPM profiles from a tachometer.

process the signal in overlapping frames to increase the time resolution. The overlayed spectrogram is shown in Fig. 13.

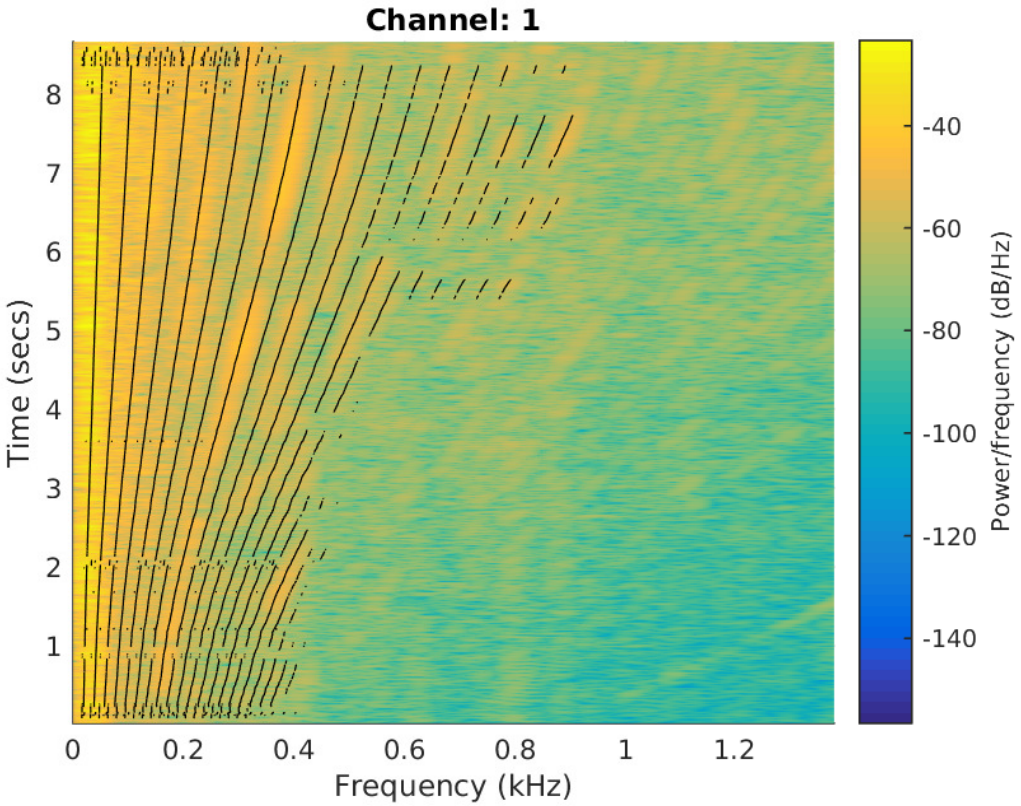

Figure 13: Spectrogram of a car engine acceleration. Settings: 2048 sample Hann window, 2000 sample overlap, $N_{\text{FFT}} = 8192$. The black lines indicates the fundamental frequency and overtones for the harmonic signal at the given time using overlap $o = 400$ and $N = 512$.

Tachometer Signal Analysis

In this section, we illustrate how we would estimate the RPM profile of an engine from a raw tachometer signal. In order to know the ground truth and to be able to predict how accurately, the rotation frequency of an engine can be estimated, we use a simulated tachometer signal. This was generated in the following way.

1. An ideal square wave signal with a duty cycle of 10 % was generated. The period of the square wave was set to 60 ms which corresponds to a rotation frequency of 1000 RPM if the tachometer generates one pulse per revolution. The square wave was sampled at a sampling frequency of 8 kHz. We refer to this signal as the *ideal tachometer signal*.

2. The ideal tachometer signal was passed through a second order low-pass Butterworth filter with a cut-off frequency at 100 Hz.

3. Noise was added to the low-pass filtered tachometer signal. In the simulations, we have used both Gaussian and Laplacian noise. The latter is much more impulsive than the former.

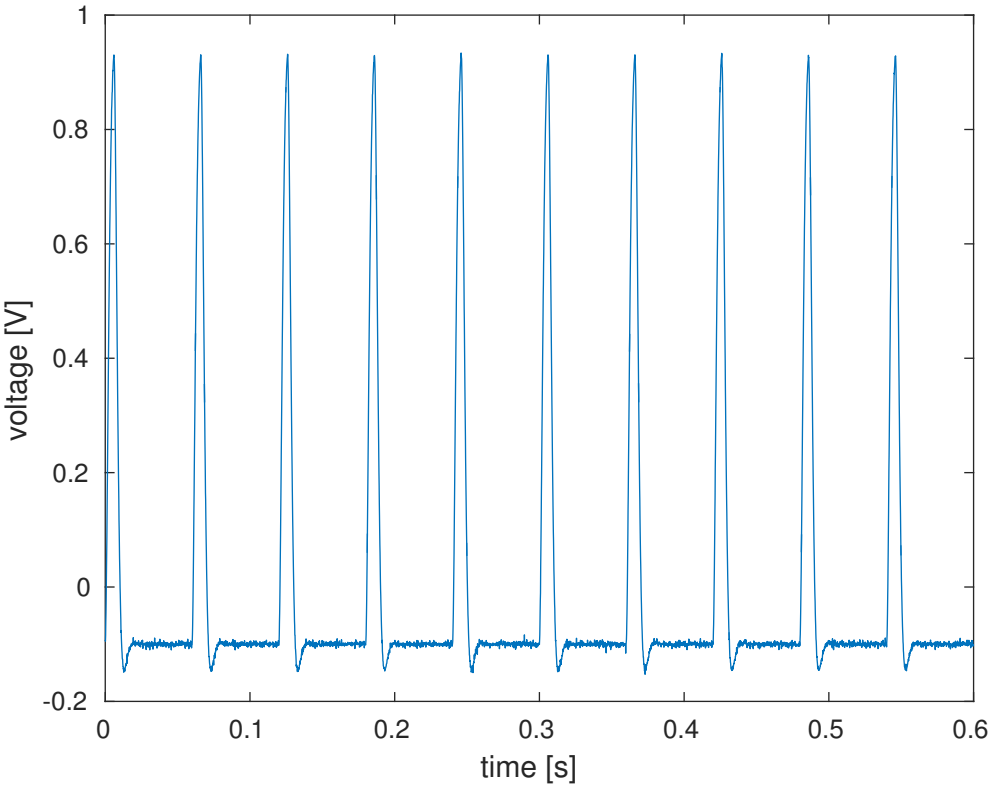

Figure 14: The simulated tacho signal for Laplacian noise and an SNR of 40 dB.

Examples of the tachometer signals for SNRs of 40 dB and 0 dB are shown in Fig. 14 and Fig. 15, respectively.

RPM Profile Estimation

Although we have not performed an exhaustive literature study, we have found that the RPM profile of an engine is typically estimated as shown in Fig. 16. In the figure, the RPM profile is estimated by estimating the distance between positive crossings of the tachometer signal with some trigger level. To make the estimator robust towards noise, a hysteresis and a hold off time can also be specified. This approach to estimating the RPM profile has not only been suggested recently in [13] and [2], but we also believe

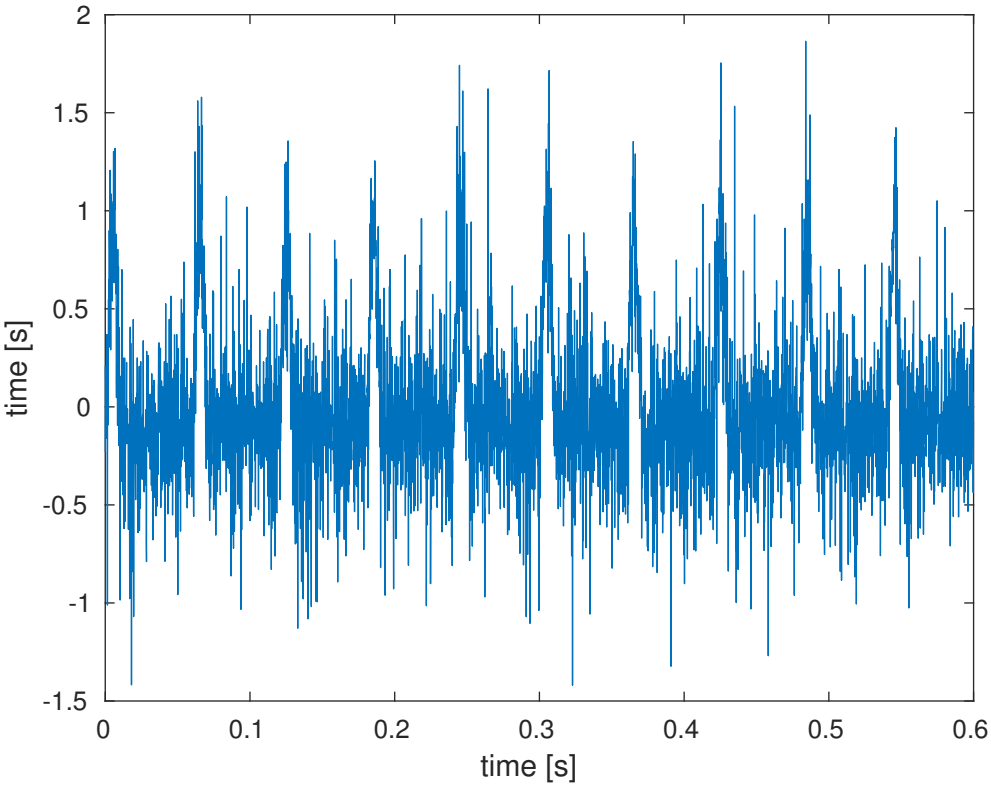

Figure 15: The simulated tacho signal for Laplacian noise and an SNR of 0 dB.

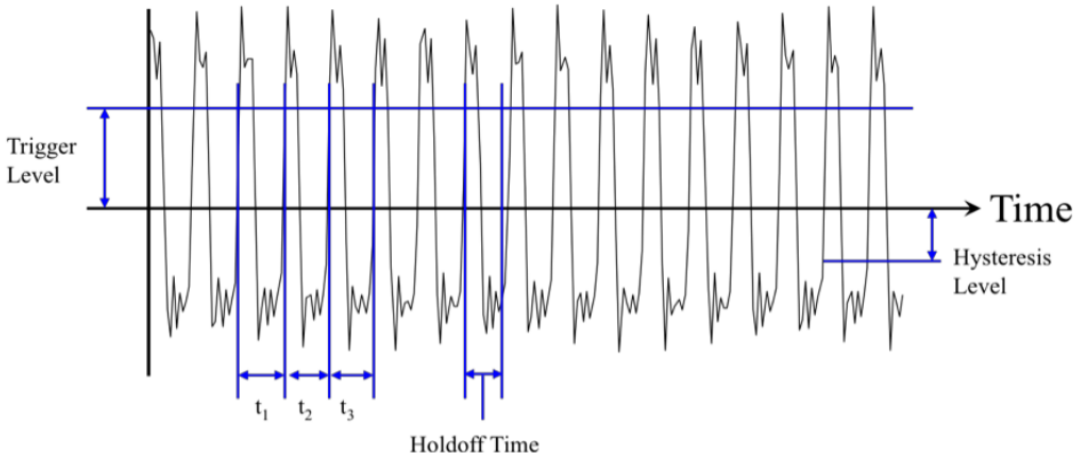

Figure 1: Example tachometer signal with processing parameters labeled.

Figure 16: Illustration of how the RPM profile of an engine is estimated from a tachometer signal [13].

that this (in a more advanced form) is used in Brüel & Kjær's PULSE Reflex software. Although the estimator may work fine for a tachometer signal as the one in Fig. 14, there are a number of problems with it.

- The low-pass filtering of the ideal tachometer signal makes the amplitude of the observed tachometer signal dependent on the rotation frequency of the engine. Thus, it might be hard to find good and global values for the user controlled trigger level, hysteresis level, and hold-off time that work across a wide range of rotation frequencies and SNRs.
- The resolution of the estimated RPM is limited to the sampling grid. To improve the resolution, the sampling frequency can be increased or interpolation can be used.
- The trigger-based estimator breaks down for impulsive noise and when the SNR is low as in, e.g., Fig. 15.

Fortunately, all of these problems can be avoided by using the ML estimator in (18). We demonstrate this below. First, however, we investigate how accurately the RPM profile can be estimated from a tachometer signal such as the one in Fig. 15. Although it may seem hopeless at first to extract the RPM profile from this signal, it is actually possible to estimate it to within an accuracy of only a few RPMs.

The Cramér-Rao Lower Bound

The Cramér-Rao Lower Bound (CRLB) is an important tool in estimation theory [14]. It gives a lower bound on the variance of any unbiased estimator and is often used for benchmarking the performance of an estimator. If we are able to find an estimator whose performance attains this bound, then we say that this estimator is statistically efficient or optimal. For the periodic signal model in (3) with $\beta_0 = 0$, it is possible to show that the variance of any unbiased estimator $\hat{r}$ of the rotation frequency is asymptotically lower bounded by

$$\operatorname{var}(\hat{r}) \geq \frac{21600 f_{\mathrm{s}}^2 \sigma^2}{\pi^2 N^3 \sum_{i=1}^{l} A_i^2 i^2} \tag{21}$$

where f_{s} and σ^2 are the sampling frequency in Hz and the noise variance, respectively. That is, it is not possible to find a unbiased estimator that has a lower variance than this. For the noise free and low-pass filtered tachometer signal we have used in this simulation study, we find that

$$\sum_{i=1}^{l} A_i^2 i^2 = 1.3857 \tag{22}$$

$$\sigma_s^2 = E[s(n)^2] = 0.0695 \tag{23}$$

where σ_s^2 is the power of the noise-free tachometer signal. By selecting the noise variance so that we get a specific SNR, we can compute this bound for a sampling frequency of

$f_s = 8000$ and $N = 1000$ data points. The results for various SNRs are shown in Table 1. From the table, we see that it actually might be possible to estimate the rotation speed for the noisy tachometer signal in Fig. 15 to within an accuracy of a few RPMs.

SNR [dB]	0	5	10	15	20	25	30	35	40
std($\hat{r}$) [RPM]	2.65	1.49	0.84	0.47	0.27	0.15	0.08	0.05	0.03

Table 1: The lower bound on the standard deviation for any unbiased estimator of the rotation frequency.

Performance of the ML Estimator

To determine how far the ML estimator (18) actually is from this bound, we ran a Monte Carlo simulation. Specifically, we generated 1000 noise realisation for every SNR and computed the root mean squared error of the estimates. Again, we used a segment length of $N = 1000$ which corresponds to a little more than two periods of the tachometer signal. The results are compared to the CRLB and shown in Fig. 17. From the figure,

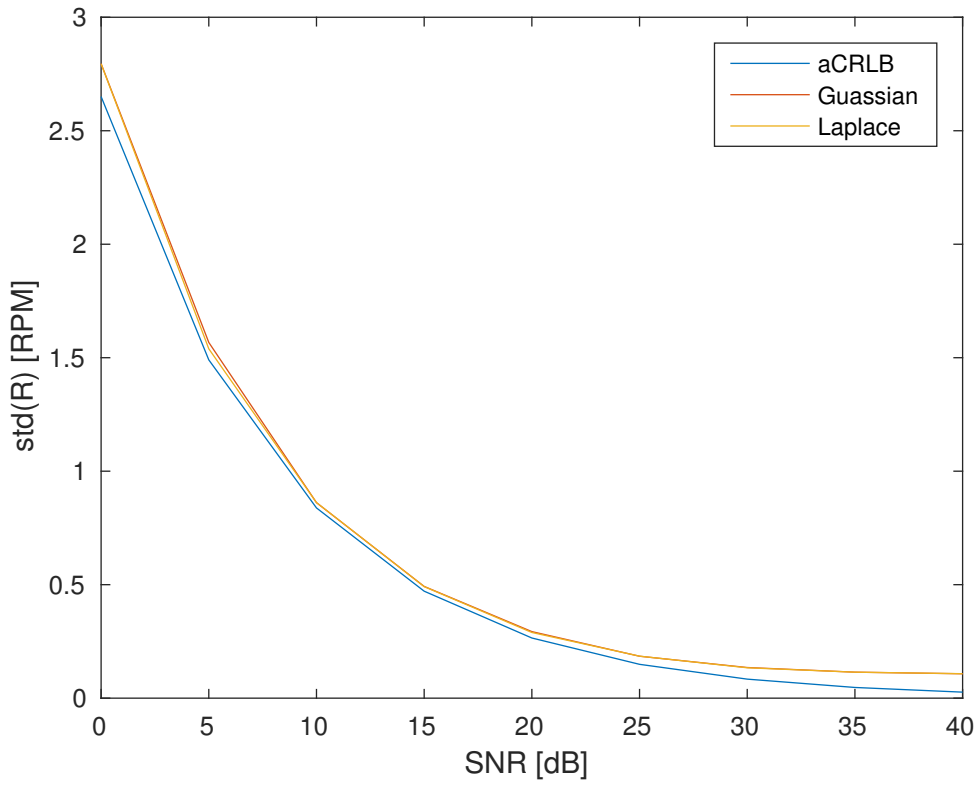

Figure 17: The root mean squared error of the ML estimator for various SNRs for both Gaussian and Laplacian noise.

we see that the ML estimator is nearly an optimal estimator despite that the simulated tachometer signal is not generated directly from the periodic signal model and that the model order l is also assumed unknown. This means that we are actually able to estimate the rotation frequency very accurately in even adverse signal conditions. Moreover, the algorithm does not require fine tuning of some user parameters to give this performance.

Is it really necessary to estimate the RPM Profile?

Today's computed order tracking methods typically feature a two step procedure.

1. Estimate the RPM profile.
2. Use the estimated RPM profile to resample the acoustic/vibrational signal and perform the analysis of the re-sampled signals.

In a parametric framework, these two steps can be combined into one. If we have both an acoustic signal $\boldsymbol{x}_\mathrm{a}$ and a tachometer signal $\boldsymbol{x}_\mathrm{t}$, then the signal model in (7) can be extended as

$$\begin{bmatrix} \boldsymbol{x}_\mathrm{a} \\ \boldsymbol{x}_\mathrm{t} \end{bmatrix} = \begin{bmatrix} \boldsymbol{H}_{l_\mathrm{a}}(\omega_0, \beta_0) & \boldsymbol{0} \\ \boldsymbol{0} & \boldsymbol{H}_{l_\mathrm{t}}(\omega_0, \beta_0) \end{bmatrix} \begin{bmatrix} \boldsymbol{\alpha}_{l_\mathrm{a}} \\ \boldsymbol{\alpha}_{l_\mathrm{t}} \end{bmatrix} + \begin{bmatrix} \boldsymbol{e}_\mathrm{a} \\ \boldsymbol{e}_\mathrm{t} \end{bmatrix} \tag{24}$$

where $\boldsymbol{e}_\mathrm{a}$ and $\boldsymbol{e}_\mathrm{a}$ have different noise variances. The ML estimator for this signal model can now be derived to

$$\begin{aligned}(\hat{\omega}_0, \hat{\beta}_0) = \underset{\omega_0, \beta_0}{\operatorname{argmin}} \ln \left[\boldsymbol{x}_\mathrm{a}^T \left(\boldsymbol{I}_N - \boldsymbol{H}_{l_\mathrm{a}}(\omega_0, \beta_0) \left[\boldsymbol{H}_{l_\mathrm{a}}^T(\omega_0, \beta_0) \boldsymbol{H}_{l_\mathrm{a}}(\omega_0, \beta_0) \right]^{-1} \boldsymbol{H}_{l_\mathrm{a}}^T(\omega_0, \beta_0) \right) \boldsymbol{x}_\mathrm{a} \right] \\ + \ln \left[\boldsymbol{x}_\mathrm{t}^T \left(\boldsymbol{I}_N - \boldsymbol{H}_{l_\mathrm{t}}(\omega_0, \beta_0) \left[\boldsymbol{H}_{l_\mathrm{t}}^T(\omega_0, \beta_0) \boldsymbol{H}_{l_\mathrm{t}}(\omega_0, \beta_0) \right]^{-1} \boldsymbol{H}_{l_\mathrm{t}}^T(\omega_0, \beta_0) \right) \boldsymbol{x}_\mathrm{t} \right]\end{aligned} \tag{25}$$

which can also be computed efficiently using our proposed fast implementation [6–8]. Compared to the two step procedure, this joint approach has a number of advantages.

- The information in both signals are used to estimate the rotation frequency.
- If the tachometer signal has a much better SNR than the acoustical signal, the tachometer signal will dominate the cost function. If, on the other hand, the tachometer signal is missing or corrupted, the acoustical signal will dominate the cost function.
- The data are combined in an optimal way seen from an estimation theoretic perspective.
- If multiple acoustical sensors are available or perhaps a mixture of acoustical and vibrational sensors, the above multichannel model can easily be extended to also include these.

Summary

In this short report, we hope to have demonstrated and analysed some of the advantages of using parametric modelling and methods for order tracking analysis. To summarise, we think that the main advantages are the following.

- A high time and frequency resolution, even at a low sampling frequency.
- The rotation frequency and number of significant orders can be estimated directly from acoustical og vibrational signals.
- Run-up and coast-downs can be included in the model using a chirp parameter β_0.
- The raw tachometer signal is also a periodic signal, and the RPM profile can therefore also be estimated accurately by analysing it in the exact same way as the acoustical og vibrational signals are analysed in parametric framework.
- The parametric framework allows us to formulate a multi-channel model for all the data (acoustical, vibrational, tachometer). An estimator based on such a multichannel model is much more robust to failures in one of the channels.
- The parametric framework can also be extended to include beamforming so that noise sources (such as tyre noise) can be filtered out spatially.
- The number of user defined parameters is typically much smaller.

We have a long list of interesing research problems in relation to extending the solutions, we already have, and to solve the problems, we have not been looking into yet.

Acknowledgement

We would like to thank Brüel & Kjær for providing the data and access to their software.

References

[1] S. Gade, H. Herlufsen, H. Konstantin-Hansen, and N. J. Wismer, "Order tracking analysis," Brüel & Kjær A/S, Technical Review No. 2, 1995.

[2] A. Brandt, *Noise and vibration analysis: signal analysis and experimental procedures*. John Wiley & Sons, 2011.

[3] S. Gade, T. F. Pedersen, H. Herlufsen, and H. Konstantin-Hansen, "Practical experience with rpm estimation using the autotracker algorithm," in *IMAC-XXV: Conference & Exposition on Structural Dynamics*, 2007.

[4] M.-C. Pan and C.-X. Wu, "Adaptive Vold–Kalman filtering order tracking," *Mechanical systems and signal processing*, vol. 21, no. 8, pp. 2957–2969, 2007.

[5] T. F. Pedersen and L. K. Hansen, "Bayesian multichannel tracking of periodic signals: A new way to detemine the running speed of mechanical systems," in *Seventh International Symposium on Signal Processing and its Applications ISSPA 2003 1-4 July 2003, Paris, France*, 2003.

[6] J. K. Nielsen, T. L. Jensen, J. R. Jensen, M. G. Christensen, and S. H. Jensen, "A fast algorithm for maximum likelihood-based fundamental frequency estimation," in *Proc. European Signal Processing Conf.*, 2015, pp. 589–593.

[7] ——, "Fast fundamental frequency estimation: Making a statistically efficient estimator computationally efficient," *Elsevier Signal Processing*, vol. 135, pp. 188–197, 2017.

[8] ——, "Fast and statistically efficient fundamental frequency estimation," in *Proc. IEEE Int. Conf. Acoust., Speech, Signal Process.*, 2016, pp. 86–90.

[9] ——, "Fast harmonic chirp summation," in *Proc. IEEE Int. Conf. Acoust., Speech, Signal Process.*, 2017, pp. 416–420.

[10] T. L. Jensen, J. K. Nielsen, J. R. Jensen, M. G. Christensen, and S. H. Jensen, "A fast algorithm for maximum likelihood estimation of harmonic chirp parameters," *IEEE Trans. Signal Process.*, 2017, accepted.

[11] J. K. Nielsen, M. G. Christensen, and S. H. Jensen, "Default Bayesian estimation of the fundamental frequency," *IEEE Trans. Audio, Speech, Lang. Process.*, vol. 21, no. 3, pp. 598–610, Mar. 2013.

[12] J. K. Nielsen, M. G. Christensen, A. T. Cemgil, and S. H. Jensen, "Bayesian model comparison with the g-prior," *IEEE Trans. Signal Process.*, vol. 62, no. 1, pp. 225–238, 2014.

[13] J. R. Blough and J. P. DeClerck, "Development of an automated order tracking method," in *Proc. Int. Conf. Noise and Vibration Eng.*, 2012, pp. 661–668.

[14] S. M. Kay, *Fundamentals of Statistical Signal Processing, Volume I: Estimation Theory*. Englewood Cliffs, NJ, USA: Prentice Hall PTR, Mar. 1993.